The Effect of Footpiece Design on the Performance of a Small Air Lift Pump

G. J. Parker†

A small air lift pump made from 24·3 mm bore glass tube has been tested with two different air injection footpiece designs. In one (the air-jacket design), air was injected radially inwards, and in the other (the nozzle design), air was injected axially at inlet to the riser. Each design has been tested using a variety of injection hole sizes and numbers. With the air-jacket design, the pump discharge characteristic was found to be independent of the number and sizes of the injection holes. The nozzle design showed greater pumping capability at high air flow rates and with small orifice area, but the efficiency was then very low. Some comparisons with the theoretical model of Stenning and Martin (9) have been made, and the model has been extended to take account of the momentum of the air injected in the nozzle footpiece.

NOTATION

A Pipe cross-sectional area
A_j Cross-sectional area of injected air jet
D Pipe diameter
E Pump Effectiveness
f Friction factor $\left(\text{defined by, head loss} = \frac{4fL}{D}\frac{V^2}{2g}\right)$
g Acceleration of gravity
H Depth of submergence
K Friction parameter $= (4fL)/D$
L Length of pump
p Pressure
Q Volume flow rate
S Slip ratio $= V_g/V_f$
V Velocity
W Weight
ρ Density
τ Wall shear stress

Subscripts

1 Entering injection zone
2 Leaving injection zone
a Atmospheric
f Liquid
g Gas

1 INTRODUCTION

Air lift pumps are very simple devices consisting of a vertical riser tube which is partially immersed in the fluid to be pumped and into which air is injected at the base to produce an upward flow. The common injector design is one in which numerous small holes are drilled radially through the pipe wall and air is supplied to them from a surrounding manifold. In this paper, this injector is called an air-jacket type.

In the early years of this century, air lift pumps were widely used for pumping water from artesian wells and from mineshafts, and for pumping in oil wells. Nowadays, air lift pumps are used mainly for specialized tasks such as aerating water, preventing icing on some high-latitude waterways, and as sea-bed 'vacuum cleaners' in underwater exploration (1). They are also sometimes used in sewage treatment plants (2).

† Senior Lecturer, Department of Mechanical Engineering, University of Canterbury, Christchurch, New Zealand
Received 17 June 1980 and accepted for publication on 27 August 1980

Much of the testing carried out in the early days and reported in the literature was undertaken on actual plant operating under normal and often varying conditions. The pumps were generally large, with submergences ranging from 30 m to 170 m and diameters ranging from 50 mm to 190 mm (3, 4, 5). No comprehensive analysis was developed, although broad conclusions about the effect of some of the variables were deduced from the experiments and simple theory (6).

Little has been reported on the effect of the footpiece design. Purchas (4) discussed several different designs, but the final selection was made on the grounds of corrosion resistance rather than pump performance. Gibson (6) briefly described tests on a pump using a nozzle type of footpiece but although efficiencies were good, no direct comparison was made with an air-jacket injector in the same pump under similar conditions. Stepanoff (7) discounted the use of nozzle air injectors because of the increased load on the compressor supplying the air.

The studies of Nicklin (8) and of Stenning and Martin (9) were significant contributions to the analysis of air lift pumps in that they applied the basic principles of two-phase flow to the pump and were able to make predictions about its performance. However, the effect of the footpiece was not considered by Nicklin, and Stenning and Martin used the 'standard' air-jacket type of footpiece. More recently, Stenning and Martin's test data have been extended, with almost identical apparatus, by Sharma and Sachdeva (10).

The tests reported in this paper were made to determine what influence the footpiece design had over the pump performance. Two types were investigated: the air-jacket injector, and a nozzle injector placed on the axis of the riser, just below the bell-mouth inlet.

2 EXPERIMENTAL EQUIPMENT

The apparatus is shown in sketch form in Figure 1. The riser was a length of 24·3 mm bore glass tube to allow observation of the flow. The various footpiece designs were fastened in turn to the flange at the bottom of the tube, and a short smooth bend of steel pipe was provided at the top to make water collection easy. The submergence depth was kept constant by overflowing the water supplied to the glass holding tank.

The two designs of footpieces tested are sketched in Figure 2, (a) and (b). Both were made from flanged copper

0142/727X/80/1200-0245$02.00

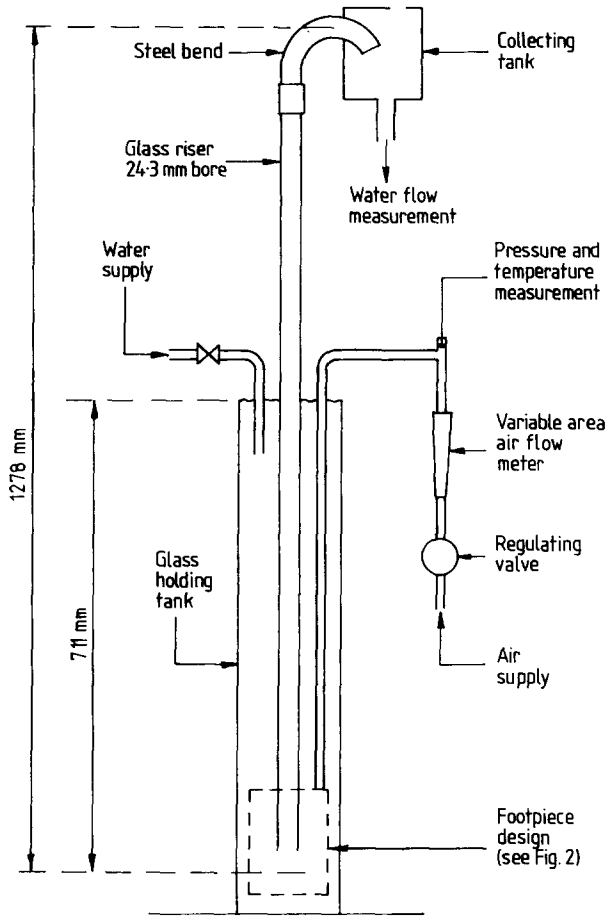

Fig. 1. Apparatus for testing the air-lift pump

tube matching the bore of the glass riser. In the air-jacket footpiece, the injection holes were drilled through the copper tube and the unit was surrounded by a larger tube forming a manifold for the air supply. Several units were made with different numbers and sizes of holes. In the nozzle footpiece, air was supplied to a small nozzle chamber located on the centre-line of the riser. A screwed cap enabled injector plates with various hole configurations to be interchanged rapidly. The hole configurations tested are listed in Table 1.

The distance of the nozzle injector below the bell-mouth was set at 10 mm after tests showed that this gave minimal restriction to the water flow, and yet did not lead to spillage of air around the bell-mouth.

Table 1
Orifice size and number combinations used in the tests

	Orifice Diameter	No. of orifices
Air-Jacket footpiece	1 mm	4, 8, 16, 32
	2 mm	4, 8, 22
	6 mm	1
Nozzle footpiece	1 mm	4, 8, 16, 24, 36
	2 mm	2, 4, 6
	6 mm	1

To be able to make meaningful comparisons between the tests, it was important to ensure that the pump always operated with the same submergence and lift. The submergence was measured as the distance between the air injection holes and the free surface in the holding tank. The resulting configuration gave a pump with a submergence of 711 mm and a total length of 1278 mm. Thus the ratio (submergence/length) was 0·556.

Air was supplied to the pump from the laboratory air-line, after passing through a pressure regulating valve and a variable area flow meter. The pressure and temperature of the air at the flow meter were recorded for calibration purposes.

3 RESULTS AND DISCUSSION

3.1 Flow Regime

No matter what size or number of injection holes were used, the bubbles generated rapidly coalesced to form slugs, so the flow patterns encountered in this study ranged from bubbly-slug flow at the lowest air flow rates at which water was pumped to slug-annular at the high air flow rates. There was no noticeable difference in the flow pattern with either footpiece. Unsteadiness in the flow frequently occurred and appeared to coincide with the bursting of the slugs of air out of the top of the tube.

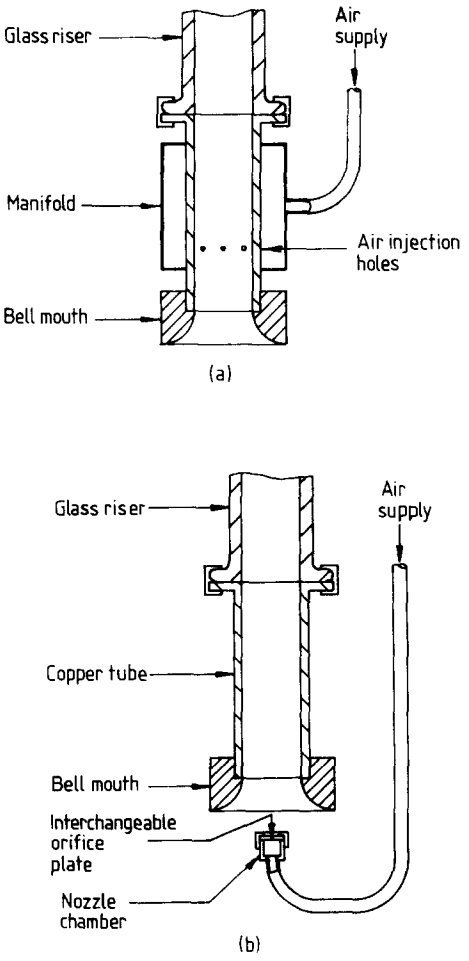

Fig. 2. Details of the footpiece designs tested. (a) the air-jacket injector, (b) the nozzle injector

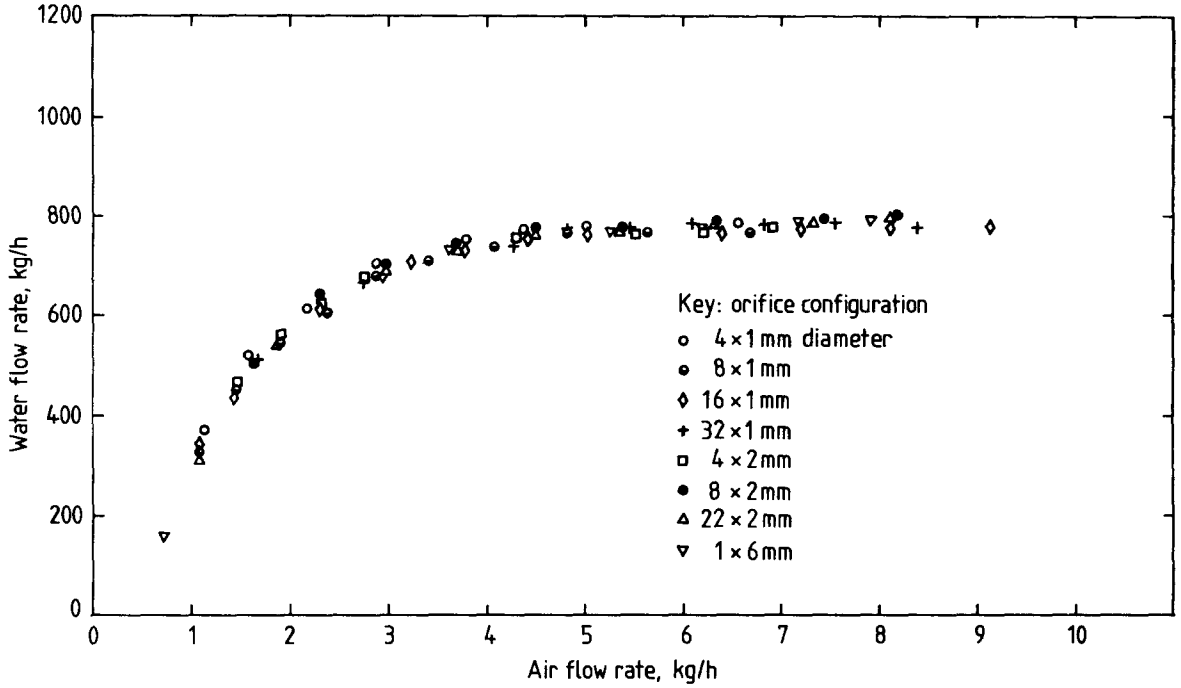

Fig. 3. Test results with the air-jacket footpiece

3.2 Discharge Characteristics

These are shown in Fig. 3 and Fig. 4 in terms of the mass flow rate of water pumped for a given air mass flow rate supplied. It is apparent that for the air-jacket footpiece the different injection hole configurations had no effect on the performance, all the experimental data tending to fall on to a common line. Insufficient air capacity was available in these tests to obtain the reduction in water flow rates at high air flow rates, obtained by other workers.

With the nozzle footpiece, the orifice area clearly had an influence on the quantity of water pumped. The smallest orifice area tested (4 × 1 mm diameter holes) gave the highest pumping rate, and the quantity continued to rise throughout the testing range. The effect was dependent only on the total orifice area, since there was minimal difference in performance for the following groups of holes: 8 × 1 mm and 2 × 2 mm diameter; 16 × 1 mm and 4 × 2 mm diameter; 24 × 1 mm and 6 × 2 mm diameter; 36 × 1 mm and 1 × 6 mm diameter. It was believed that the increased pumping capability was due to the initial momentum of the air issuing from the orifices, and this is discussed further below.

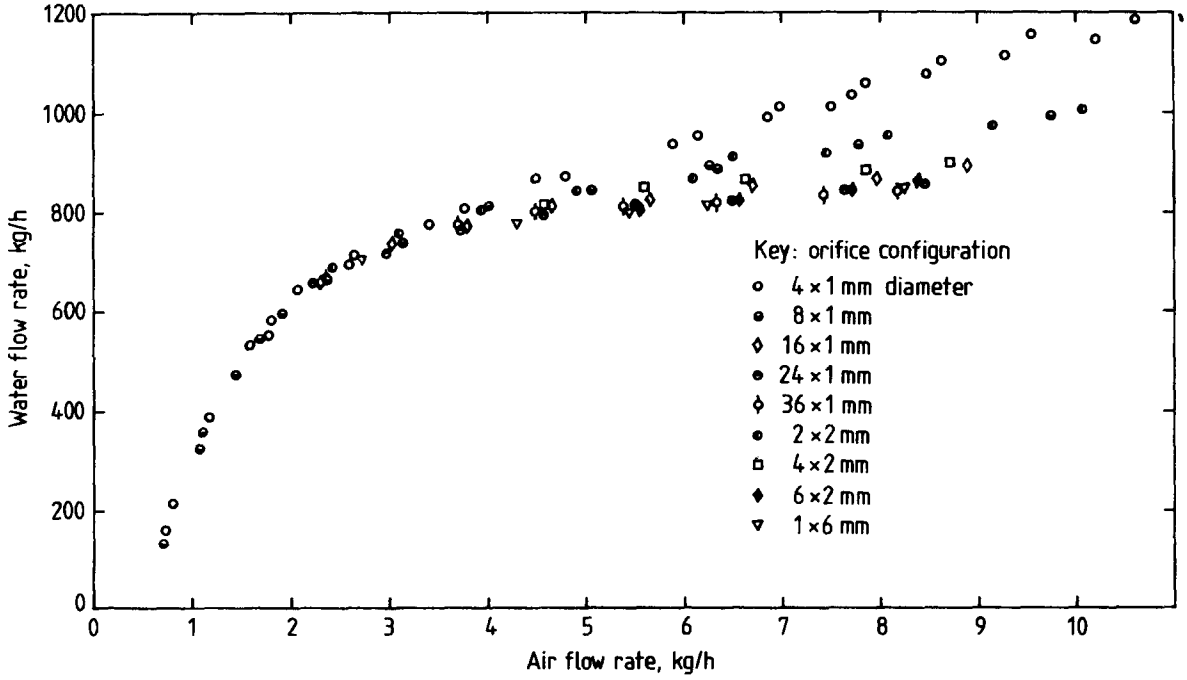

Fig. 4. Test results with the nozzle footpiece

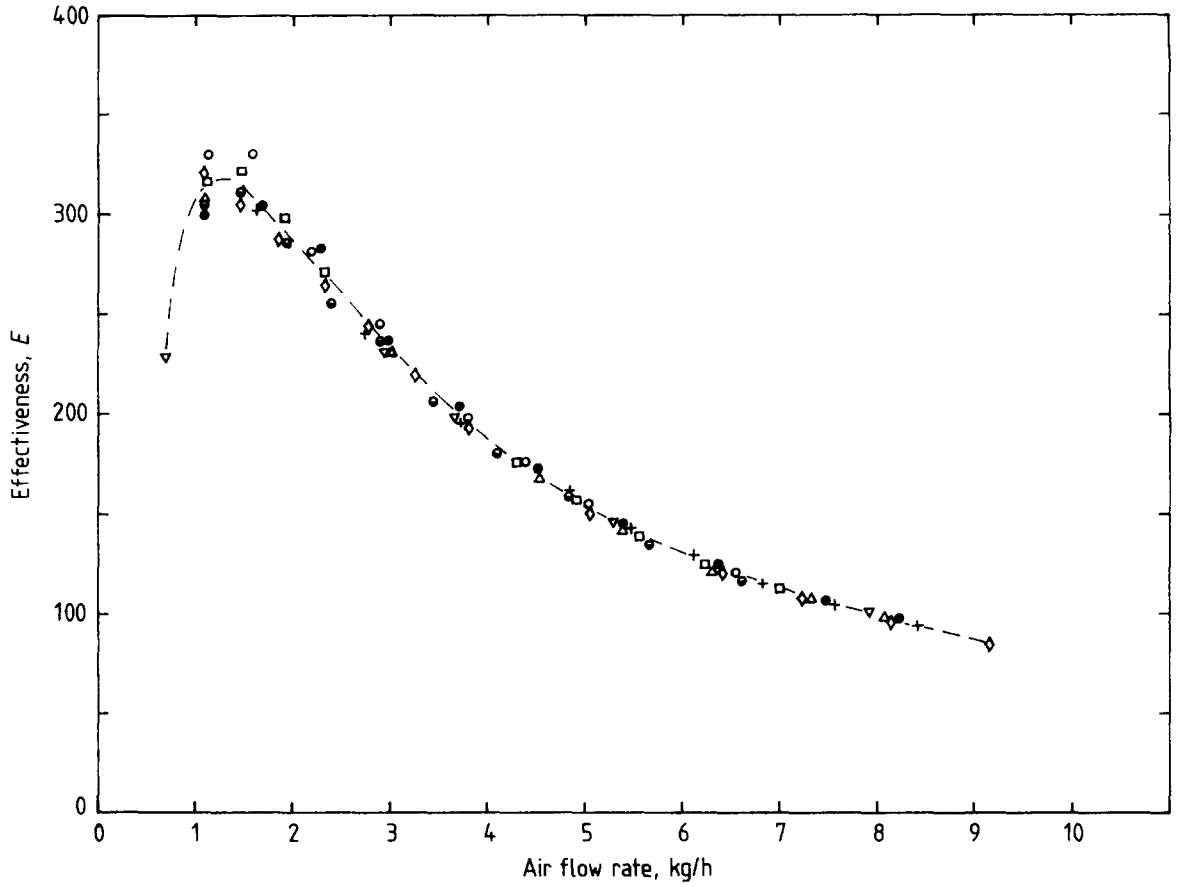

Fig. 5. The variation of pump effectiveness with air flow rate–air-jacket footpiece. The effectiveness is defined as $E = \rho_f Q_f / \rho_g Q_g$. Key as in Fig. 3

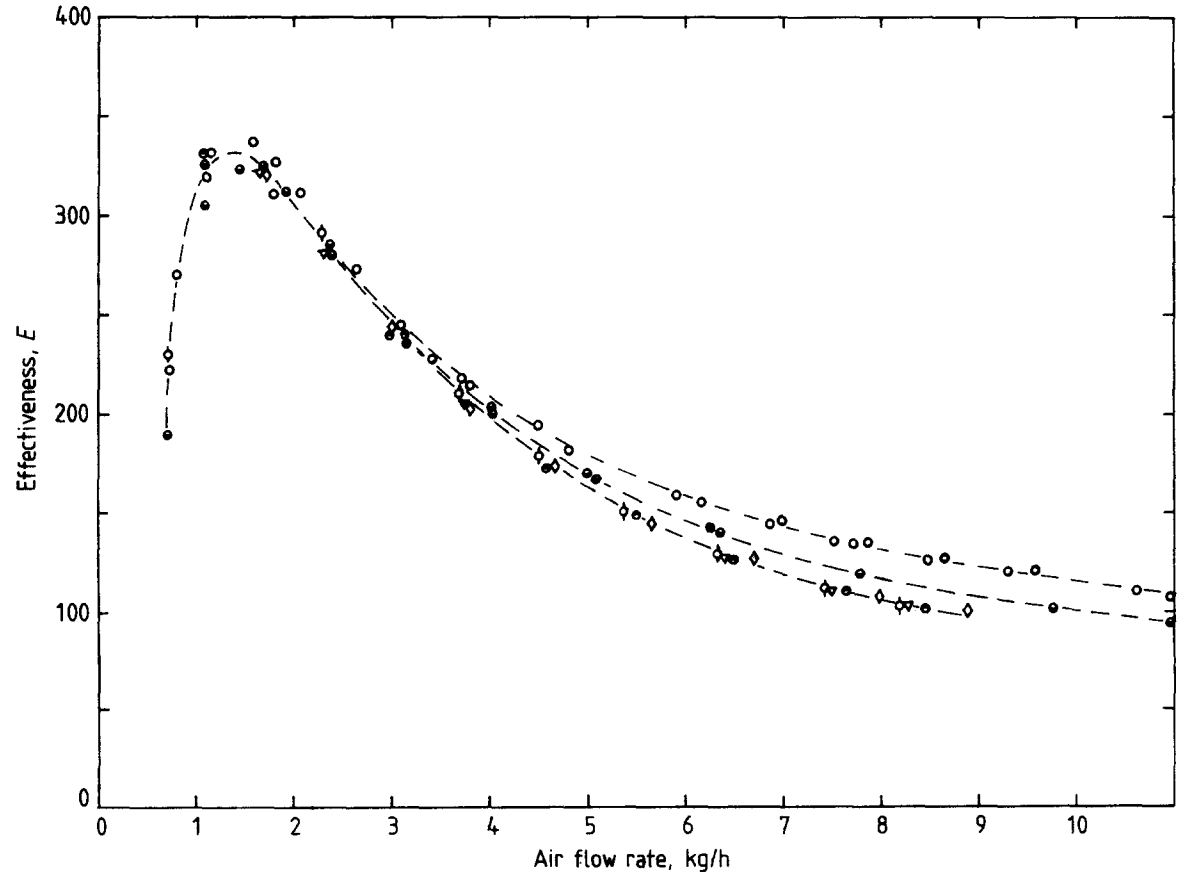

Fig. 6. The variation of pump effectiveness with air flow rate–nozzle footpiece. Key as in Fig. 4

3.3 Effectiveness and Efficiency

In comparing the performance of the pump with each footpiece it was necessary to remove the effect of the different pressure losses in the air-lines leading to the manifold and chamber behind the orifices. (Manifold pressures were not recorded.) A suitable parameter for comparison was the mass of water pumped per unit mass of air supplied, here termed the Effectiveness, E, and this is plotted in Fig. 5 and Fig. 6.

The effectiveness with the air-jacket footpiece reached a peak of approximately 320 at the comparatively low air flow rate of 1·25 kg/h (this point corresponds to the point on the discharge curve where a line through the origin is tangent to the curve). At higher air flow rates, more water was pumped, but with a much lower effectiveness.

With the nozzle footpiece, the effectiveness peak value was approximately 330 at an air flow rate of 1·3 kg/h. It can be seen that the improvement in discharge characteristic with small orifice area occurred in the region of low effectiveness.

To obtain the efficiency of the pump, account had to be taken of the work input required to create the air flow through the orifices at the depth of the footpiece. Clearly the highest efficiency would be obtained when the total orifice area was the greatest. Efficiency values could not be obtained directly since the manifold pressures were not measured in these tests. However, by calculating the pressure drops across the orifice area, the work input into the air and hence the efficiency could be estimated and values are shown in Fig. 7. It should be noted that the peak in the efficiency curve does not necessarily occur at the same air flow rate as that for maximum effectiveness because of the way in which the input power varied with air flow rate.

The penalty paid by using the nozzle footpiece with small orifice area to obtain improved discharge is even more marked in terms of this calculated efficiency as seen in Fig. 7. When using 4 × 1 mm diameter holes the efficiency is less than 1 per cent for air flows greater than 4 kg/h, whereas the peak value is 14 per cent.

3.4 Comparison with the Stenning and Martin Theoretical Model

3.4.1 *Air-jacket footpiece* Stenning and Martin's model (**9**) applies directly to the air-jacket footpiece. The final equation from their analysis was

$$\frac{H}{L} - \frac{1}{\left[1 + \frac{1}{S}\cdot\frac{Q_g}{Q_f}\right]} = \frac{Q_f^2}{2gLA^2}\left[(K+1) + (K+2)\frac{Q_g}{Q_f}\right] \quad (1)$$

K is a friction parameter $= (4fL)/D$ in which the friction factor, f, in the model was to be that appropriate to the total volume flow rate flowing as liquid.

The prediction from this equation can be conveniently represented by plotting the dimensionless quantities $Q_f/[A\sqrt{(2gL)}]$ against Q_g/Q_f. The curve obtained is a function of the values chosen for the slip S and the friction

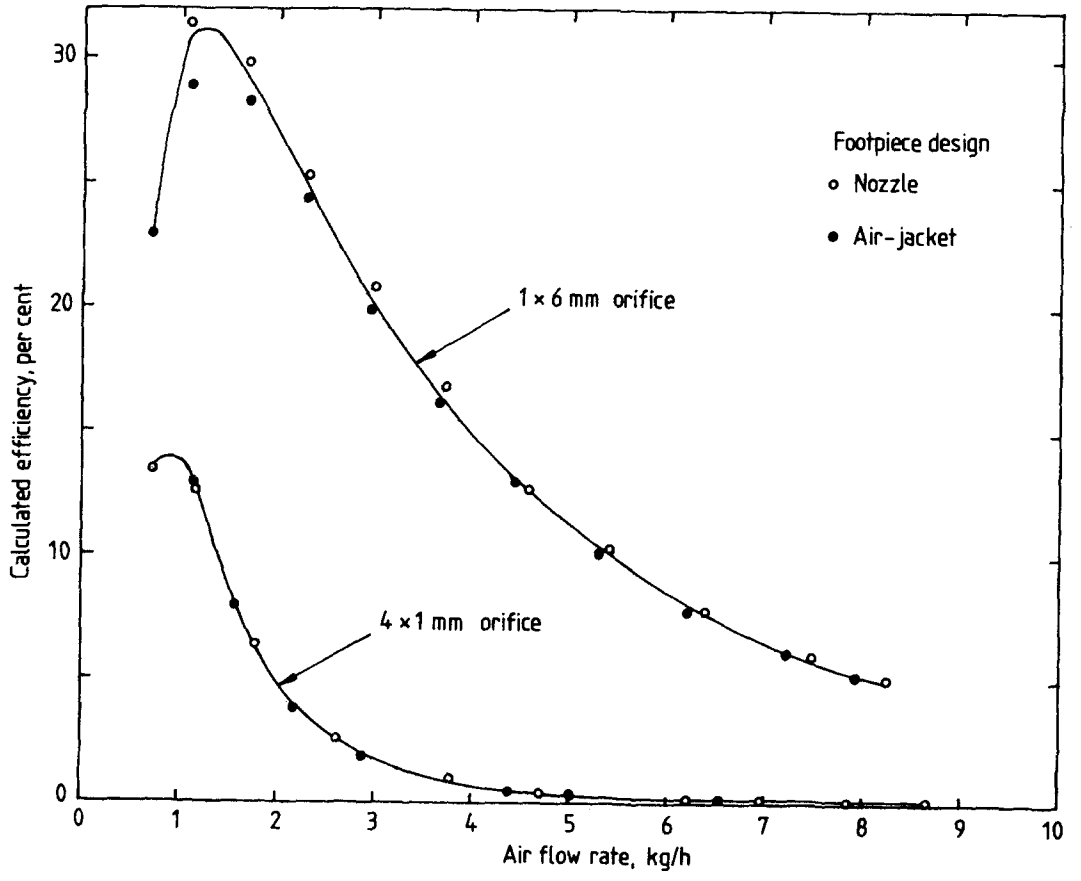

Fig. 7. The efficiency of the pump (power output in water ÷ power input in air) with different footpiece designs. The power input in the air was obtained by calculating the pressure drop across the orifices at each mass flow rate

parameter K. These parameters influence the curve differently, the slip affecting mainly the location of the intercept on the Q_g/Q_f axis and K affecting the curves mainly in the $Q_f/[A\sqrt{(2gL)}]$ direction. By plotting the experimental data in the dimensionless form, and comparing the model prediction for various values of S and K, it was found that the best fit for most of the data points was obtained using $S = 3{\cdot}0$ and $K = 1{\cdot}7$, as shown in Fig. 8. A value of $K = 1{\cdot}7$ corresponds to a friction factor f of 0·0081. Although this value is much higher than that required by the theory (as it also was in Stenning and Martin's paper), it is close to the value obtained by assuming the whole *mass* flow rate, rather than total volume flow rate, flows as liquid. This gives a useful way of obtaining approximate values for the friction factor.

Figure 8 also reveals that the Stenning and Martin model fails to predict the reversal of the curve at low air flow rates. This reversal must occur since $Q_g/Q_f \to \infty$ as $Q_f \to 0$ (Q_g is not zero for zero Q_f). This failure arises from the use of a constant value for slip. In reality, the slip must vary. As the air flow rate is reduced, the slip increases rapidly until, when no water is pumped, $S = \infty$. At high air flow rates, the quantity of water remains constant or reduces, so slip must increase with increasing air flow rate. The model therefore, when used with constant slip values, does not predict a point of operation giving maximum efficiency.

A model allowing for varying slip (and varying friction parameter K) is currently being investigated.

3.4.2 *Nozzle footpiece* The model of Stenning and Martin has been extended in this study to apply to a nozzle injector by taking account of the initial momentum of the air at inlet as it issued from the injection orifice (see Appendix). If the injector is assumed to be so small that it causes negligible blockage in the riser, then an equation identical to eq. (1) but with an extra term results, as follows:

$$\frac{H}{L} = \frac{1}{[1 + (1/S) \cdot (Q_g/Q_f)]} = \frac{Q_f^2}{2gLA^2}\left[(K+1) + (K+2)\frac{Q_g}{Q_f} - 2\frac{\rho_g}{\rho_f}\frac{A}{A_j}\left(\frac{Q_g}{Q_f}\right)^2\right] \quad (2)$$

where A_j is the cross-sectional area of the air jet at inlet.

The prediction from this equation can also be represented by using the same dimensionless parameters as for eq. (1). When eq. (2) was compared with the data from the tests with the smallest orifice area (4 × 1 mm diameter holes), it was found to overpredict the quantity of water pumped. This was not surprising since in the tests the air was injected not within the riser as modelled but 10 mm below the bell-mouth. It was found that by taking 0·52 of the additional momentum term, reasonable correlation (apart from the curve reversal, as mentioned in 3.4.1 above) was obtained, as shown in Fig. 9.

4 CONCLUSIONS

It has been found that the discharge characteristic of the air lift pump with the air-jacket footpiece was independent of the number and sizes of air injection holes.

A peak effectiveness (and efficiency) occurred at a comparatively low air flow rate, and the highest efficiency was obtained with the greatest total orifice area. The peak, which is the desirable operating point, was not predicted by the theoretical model of Stenning and Martin when constant values for slip were used.

It was possible to increase the quantity of water pumped by using a nozzle injector with small orifice area,

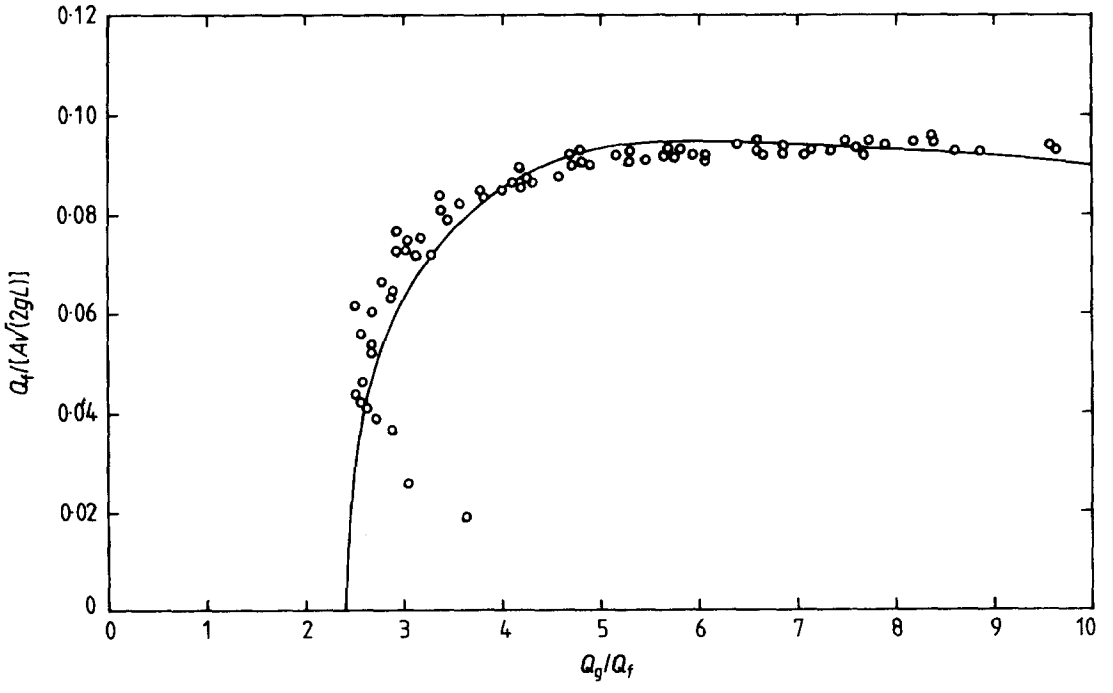

Fig. 8. Dimensionless plot of pump performance with air-jacket footpiece. Circles are experimental data, line is Stenning and Martin's theoretical model with $S = 3{\cdot}0$, $K = 1{\cdot}7$

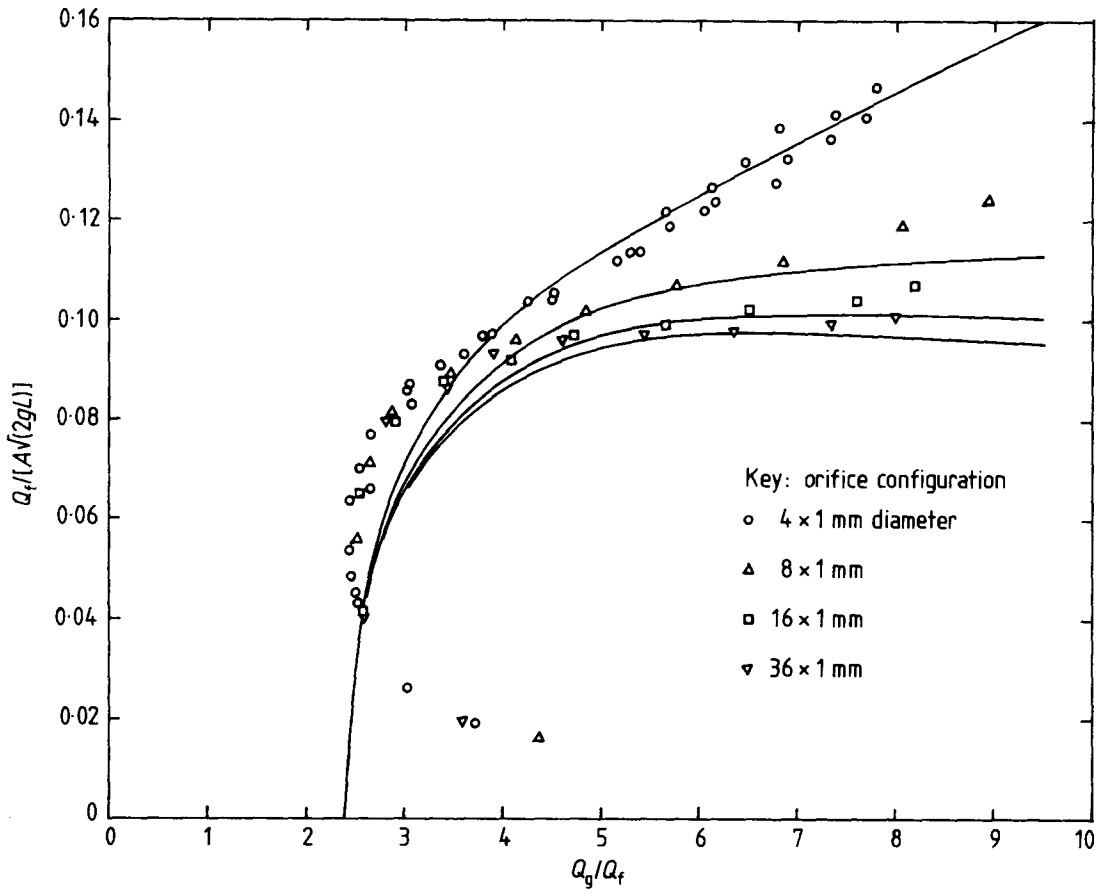

Fig. 9. Dimensionless plot of pump performance with nozzle footpiece. Circles are experimental data, lines are from the model described in the text

but the pump then operated with low effectiveness (and efficiency).

The effect of the air initial momentum in the nozzle footpiece could be predicted through an extension to the theoretical model of Stenning and Martin.

REFERENCES

(1) ANDEEN, G. B. 'Bubble Pumps', *Compressed Air* 1974, Jan
(2) BARTLETT, R. E. *Pumping Stations for Water and Sewage* 1974 (Appl. Sci. Pubs., London)
(3) MAXWELL, W. H. 'Raising Water by Compressed Air', *Engineering* 1903, **76**, 675
(4) PURCHAS, A. W. 'Some Notes on Air Lift Pumping', *Proc. Instn mech. Engrs* 1917, **93**, 613
(5) PICKERT, F. 'The Theory of the Air Lift Pump', *Engineering* 1932, **134**, 19
(6) GIBSON, A. H. *Hydraulics and Its Applications* (3rd. Ed.) 1925 (Constable & Co, London)
(7) STEPANOFF, A. J. 'Thermodynamic Theory of the Air Lift', *Trans. ASME* 1929, **51**, 49
(8) NICKLIN, D. J. 'The Air Lift Pump: Theory and Optimisation', *Trans. Instn chem. Engrs* 1963, **41**, 29
(9) STENNING, A. H. and MARTIN, C. B. 'An Analytical and Experimental Study of Air Lift Pump Performance', *J. of Engng for Power, Trans. ASME*, Series A 1968, **90** (2), 106
(10) SHARMA, N. D. and SACHDEVA, M. M. 'An Air Lift Pump Performance Study', *Instn Engrs (India) J.* 1976, **56**, 61

APPENDIX

Extension of Stenning and Martin's theoretical model to account for air initial momentum with nozzle injection

This analysis follows that of Stenning and Martin (**9**) with the modification that here the air is injected axially in plane (1) of the injection zone, see Fig. 10. The analysis applies the momentum equation (a) to the injection zone, and (b) to the remainder of the riser.

(a) The Injection Zone

By Bernoulli's equation, the static pressure at inlet to the injection zone may be written as

$$p_1 = p_a + \rho_f g H - \tfrac{1}{2}\rho_f V_1^2 \qquad \text{(A1)}$$

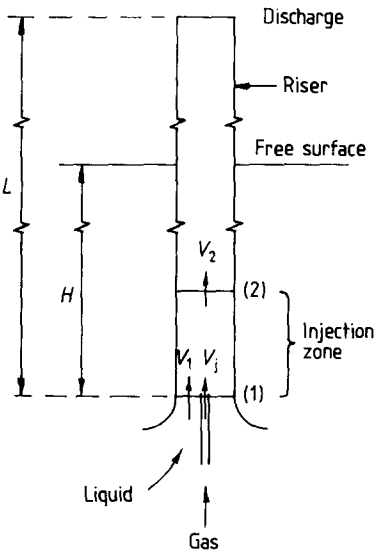

Fig. 10. Model for analysis of air lift pump with nozzle air injection

If the density change of the air in the injection zone is negligible, then the mixture velocity V_2 at (2) may be written as

$$AV_2 = Q_f + Q_g$$

But $Q_f = AV_1$, if A_j is negligible in comparison with A, so

$$V_2 - V_1 = \frac{Q_g}{A} \tag{A2}$$

The axial momentum equation for the injection zone is

$$Ap_1 - Ap_2 = (\rho_g Q_g + \rho_f Q_f)V_2 - \rho_f Q_f V_1 - \rho_g Q_g V_j$$

If $\rho_g Q_g \ll \rho_f Q_f$, as is usual, then the equation becomes

$$p_1 - p_2 = \rho_f \frac{Q_f}{A} V_2 - \rho_f \frac{Q_f}{A} V_1 - \rho_g \frac{Q_g}{A} V_j \tag{A3}$$

Combining eqs (A2) and (A3)

$$p_2 = p_1 - \rho_f V_1 \frac{Q_g}{A} + \rho_g \frac{Q_g}{A} V_j \tag{A4}$$

Substituting eq. (A4) into (A1) gives

$$p_2 = p_a + \rho_f g H - \tfrac{1}{2}\rho_f V_1^2 - \rho_f V_1 \frac{Q_g}{A} + \rho_g \frac{Q_g}{A} V_j \tag{A5}$$

The last term on the right-hand side is the extra term due to the initial momentum of the air. Since $Q_f = AV_1$ and $Q_g = A_j V_j$, eq. (A5) may be written as

$$p_2 = p_a + \rho_f g H - \tfrac{1}{2}\rho_f V_1^2 - \rho_f V_1^2 \frac{Q_g}{Q_f} + \rho_f V_1^2 \frac{\rho_g}{\rho_f} \cdot \frac{A}{A_j}\left(\frac{Q_g}{Q_f}\right)^2 \tag{A6}$$

(b) The riser

Here, the pressure force balances the wall friction and the weight of the column of fluid. The axial momentum equation is

$$p_2 - p_a = \tau \frac{L\pi D}{A} + \frac{W}{A} \tag{A7}$$

The weight of the fluid in the column is equal to the weight of the two components, and was shown by Stenning and Martin to be

$$\frac{W}{A} = \frac{\rho_f g L}{[1 + (1/S) \cdot (Q_g/Q_f)]} \tag{A8}$$

where $S = V_g/V_f$, the slip.

The wall shear stress for slug flow was given as

$$\tau = f \frac{\rho_f}{2}\left(\frac{Q_f}{A}\right)^2 \left(1 + \frac{Q_g}{Q_f}\right) \tag{A9}$$

where f is to be determined assuming that water alone flows at the total *volume* flow rate $(Q_g + Q_f)$.

Substituting eqs (A8) and (A9) into (A7) leads to

$$p_2 = p_a + \frac{4fL}{D}\frac{(\rho_f V_1^2)}{2}\left|1 + \frac{Q_g}{Q_f}\right| + \frac{\rho_f g L}{[1 + (1/S) \cdot (Q_g/Q_f)]} \tag{A10}$$

(c) The Complete Pump

Combining eqs (A6) and (A10) and re-arranging, leads to

$$\frac{H}{L} - \frac{1}{[1 + (1/S) \cdot (Q_g/Q_f)]} = \frac{Q_f^2}{2gLA^2}\left|(K+1) + (K+2)\frac{Q_g}{Q_f} - 2\frac{\rho_g}{\rho_f} \cdot \frac{A}{A_j}\left(\frac{Q_g}{Q_f}\right)^2\right| \tag{A11}$$

where $K = (4fL/D)$.

The area of the jet A_j may be related to the area of the nozzle orifice A_N through the contraction coefficient. For the geometry in these tests

$$A_j = 0{\cdot}63\ A_N \tag{A12}$$